Immuno-Fluorescence Scanning Electron Microscopy of Biological Cells

Phyllis J. Fisher,* William S. Wessels, Allan B. Dietz, and Franklyn G. Prendergast
Mayo Foundation, Rochester, MN
* fisher.phyllis@mayo.edu

Introduction

Scanning electron microscopy (SEM) can produce striking three-dimensional images of biological cells and tissues with submicron resolution of surface morphology. Such cell surfaces are often complex blends of folds, extrusions, and pockets that may be necessary in the positioning of specific molecules within interaction range of each other. Thus, surface changes can have a spatial control over some molecular functions, and identification of select molecules at distinct morphological locations becomes critical to our understanding of total cell function.

Immuno-electron microscopy has recently evolved into a well-defined area of study with the use of colloidal metal nanoparticles [1–3]. The colloids, which can be conjugated to antibodies, are available in a variety of metals and sizes that have been shown to distinguish between two specific antibody binding sites [4]. A natural extension of this line of study is the use of antibody-bound fluorophores, which are widely available in an extensive range of both antibody specificity and fluorescence emission wavelengths, and which can be excited to an emissive energy level by the electron beam of an SEM [5]. Such light production, resulting from bombardment of luminescent material by an electron beam, is called cathodoluminescence (CL).

In the field-emission gun scanning electron microscope (FEG-SEM) an electron emission current is produced by an electric field concentrated at the sharp metal tip of the gun cathode (Figure 1). The electron beam is accelerated down the column through a series of electromagnetic lenses and apertures, most of which are adjustable to some degree. This electron beam can provide over a thousand times the energy necessary to excite a fluorescent molecule. The absorbance spectra of biological materials is similar, whether excitation is by electrons or photons—as in laser excitation in confocal microscopy [6].

The photon collector consists of a focusing mirror (Figure 1, M) set either annular to, or at an angle near, the opening of the objective lens. Light emitted by the sample is collected by this mirror and piped (L) to a photomultiplier tube (PMT). Filters or a monochromator may be placed in the light path before the PMT. When the photon detector is independent of the secondary or backscatter detectors, concurrent images may be collected.

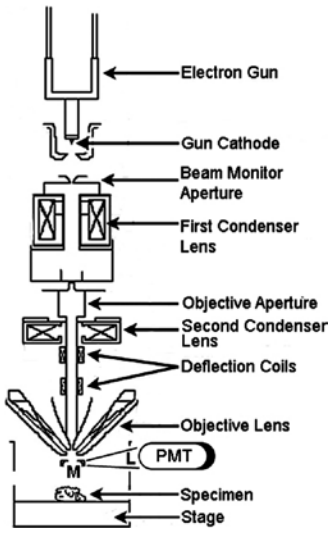

Figure 1: Diagram of a field emission gun, scanning electron microscope with cathodoluminescence attachments. (M) Light-gathering mirror, (L) light pipe connecting mirror, and (PMT) photomultiplier tube.

Detection of photons during SEM imaging has been a standard technique in geology and some materials work for several decades [7], yet it only began to emerge in the biological field since 1974 [8]. Within the last several years, development of biologically active fluorophores has exploded with a variety of over 600 currently available [9]. Today there are both primary and secondary antibodies, fluorescently labeled, with fluorescence efficiency and photostability greatly improved since their initial appearance [10, 11]. We find the relatively new semiconductor fluorophore, the quantum dot, the most useful in cathodoluminescence for its excellent quantum yield and especially for its stability under the electron beam [12].

Nevertheless, cathodoluminescence still poses several problems for biological samples, including the reduction of background autofluorescence and dispersal of surface charges without quenching the fluorescence of the antibody label. We have developed techniques and protocols to overcome these difficulties and to maximize SEM detection of photon emission from specifically labeled proteins on biological cells. To illustrate this protocol we present here images from our work in the field of human glioblastomas (brain tumors).

Cell Handling and Labeling

Glioblastomas release microvesicles (exosomes) consisting of 50- to 500-nm diameter packets of tumor cell material that contain the protein EGFr (epidermal growth factor receptor) [13]. We collected the supernatant from a glioblastoma cell culture, centrifuged it to remove whole cells, and then incubated it with $CD14^+$ monocytes, an immune system precursor to dendritic cells, which have been shown to accumulate near tumors [14] and which do not express EGFr [15]. After several hours the monocytes, which were fixed and washed, were labeled with an antibody to EGFr and a secondary antibody conjugated with fluorescent quantum dots. Simultaneous fluorescence and electron imaging of these monocytes delineated specifically labeled glioblastoma exosomes, which attached to the veil-like membrane extensions of the cell (Figure 2).

The CD 14^+ mononuclear cells (monocytes) were isolated by negative selection immunoadsorption from human peripheral blood [16]. For those experiments involving tumor exosomes, the monocytes were incubated at 37°F, 5% CO_2, with the supernatant of a U373 glioblastoma cell culture for two or more hours. Since biological samples for SEM imaging must be fixed and dried thoroughly, particular care must be taken toward maintaining the fluorescence of attached labels

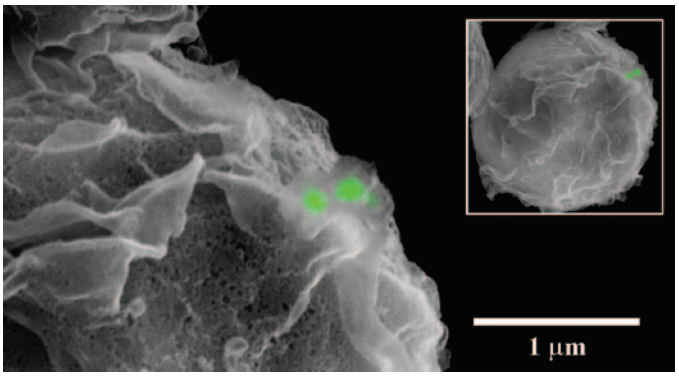

Figure 2: U373 glioblastoma exosomes labeled with Qdot 565 bound to anti-EGFr (see Cell Handling & Labeling) (green) are bound to the membrane veil of a monocyte of the immune system. The electron image (gray-scale), from a mix of the upper and lower electron detectors, is overlaid with the CL image (green). (Inset) The cell from which the enlargement was taken.

while avoiding an increase in autofluorescence [17]. We use fresh, buffered, pH 7.4, room temperature, formaldehyde (2%) for 30–45 minutes [each cell type should be tested for optimal fixation techniques], followed by a buffer wash using slow pipetting. The supernatant/monocyte samples were labeled with mouse anti-human EGFr (Invitrogen, Carlsbad, CA) and secondarily labeled with goat anti-mouse Qdot 565 (Invitrogen). Some monocytes were labeled, straight from the isolation procedure, with mouse anti-human CD14 (Invitrogen) and secondarily labeled with goat anti-mouse Qdot 605 (Invitrogen). In the case of these experiments, we used Qdots as secondary labels because the primary labels had been obtained for other experimental applications. Spatial resolution will, of course, be improved with the use of only primary labels. The monocytes prepared for confocal imaging were handled just as those used for the exosome/monocyte cathodoluminescence except that CMFDA, a cytoplasmic dye (Invitrogen), was added to the monocytes before incubating with the tumor supernatant.

Sample Preparation

Generally, SEM samples are sputter-coated with gold/palladium (or similar metals) to avoid a charge build-up on the sample surface and subsequent saturation of the electron detector. However, like other workers [7, 18–20], we have noted almost complete loss of fluorescence with a 60-second gold/palladium coating. We found that a 15-second sputter coating passes at least 50% of the maximum fluorescence. To reduce surface charging while reducing the extent of gold coating, we mount samples on aluminum dishes. The dishes we use (ScienceGear.com, P/N MWD-3500) fit into the wells of a 24-well culture plate and are approximately the same diameter as the aluminum studs commonly used on SEM stage mounts (Figure 3). Cell culturing, labeling, fixing, and drying can all be done in the aluminum dish. After fixing and drying the cells, we affix the dish to the stud with a double-stick carbon spot, flange the edge of the dish with a small clipper, and fold down the edges to make a tight contact with the stud to ensure charge dispersal.

The ethanol wash prior to critical point drying [21] must also be kept to a minimum time to avoid membrane loss

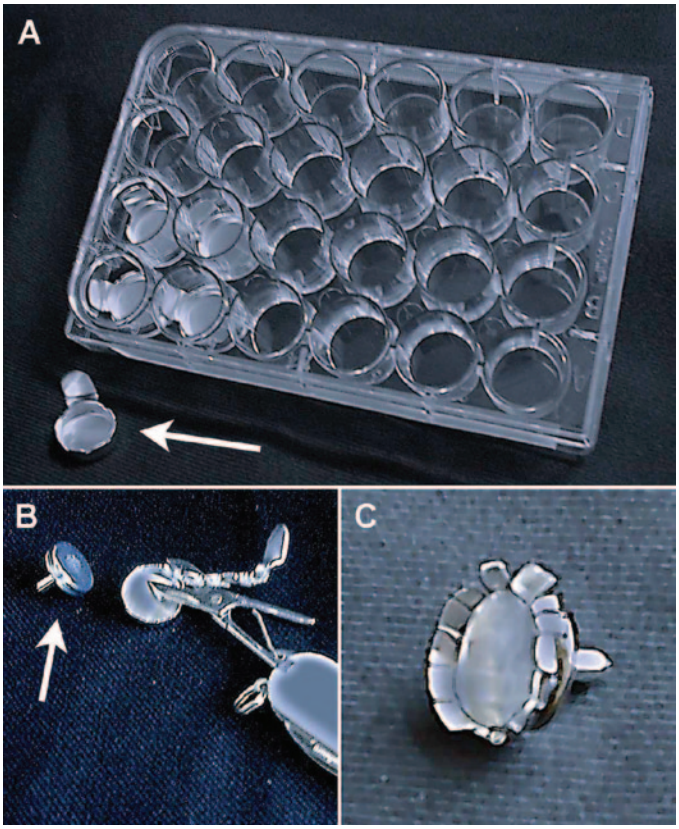

Figure 3: Aluminum dishes used for mounting, fixing, and coating cells (A). Dishes (arrow) fit into 24-well culture plates for cell growth incubation and are coated with poly-L-lysine or a similar cell growth binder to attach cells to the surface; tabs are convenient for lifting out dishes. (B) After cell processing, prior to the drying protocol, tabs and sides of dishes are trimmed and then attached to standard aluminum stage stubs (arrow) by double-sided adhesive carbon tape. (C) Flanges are cut into the side of the dish and bent under for maximum grounding contact with the stud.

and, thus, loss of surface markers. Usually the ethanol wash is performed in multiple steps of increasing ethanol concentration. We try to limit the step-up of ethanol to one or two minutes per step followed as quickly as possible by the critical point dryer.

Instrumentation

A Hitachi S-4700 FE-SEM (Hitachi, Schaumburg, IL) was used in the dual imaging mode, collecting secondary (SE) and backscattered (BS) electrons on the two built-in electron detectors and collecting photons on the Centaurus cathodoluminescence detector (KE Developments Ltd, Cambridge, UK). Of particular importance is the use of a setting on the Hitachi S-4700 termed "analysis mode," which changes the cross-over of the beam to a larger cross section, increasing the beam current about 10-fold, at the expense of some loss in image resolution. The condenser lens notch should be set to as small a value as possible consistent with an acceptable SE resolution (This setting is the negative logarithm of the specimen beam current, thus yielding a higher current from a lower notch number. We use a setting of 4.) Under this mode we use an accelerating voltage of 30 kV and an emission current starting at 40 µA, either or both of which may be decreased if the photon output of the fluorophore is high enough. Accelerating

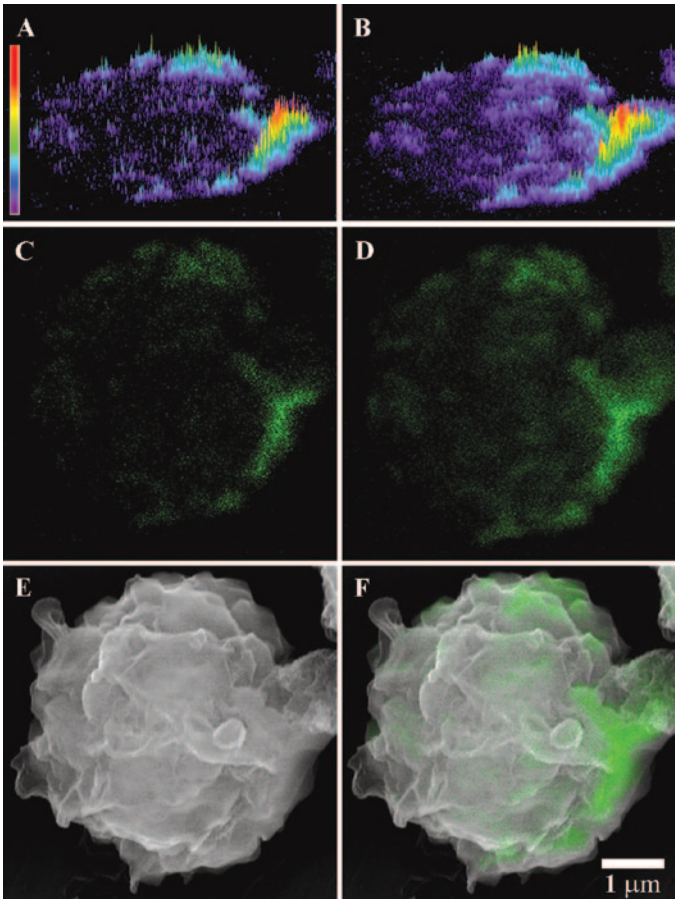

Figure 4: A monocyte (grayscale) containing tumor cell exosomes labeled with Qdot 565 bound to anti-EGFr (green) imaged at two different probe current levels, demonstrating intensity and signal concentration dependence on probe current. The exosomes (usually 50- to 500-nm diameter) on this cell have apparently fused into large masses, typical of membrane vesicular action [27]. (A) Intensity scale bar (Red = Max., Violet = Min.). Scaled intensity image of (C) with a vertical 45° tip backward. (B) Scaled intensity image of (D). (C) CL image with 20 µA probe current. (D) CL image with 37 µA probe current. (E) Secondary electron image from the upper detector. (F) Overlay of D & E. Scale bar = 1 mm.

voltage affects the size of the interaction volume (and, thus, the depth of penetration) as well as the CL intensity. A higher probe current results in a larger spot (beam) size, which yields a CL image with a higher intensity and concentration of signal [22] (Figure 4). Reduction of either of these parameters will reduce the possibility of damage to the fluorophore and the biological sample. A more efficient light-gathering system than the one used here is available (Gatan, Inc., Warrendale, PA). That instrument includes an annular parabolloidal mirror, a high-efficiency PMT, and is also available with either a monochromator or filters for multi-color imaging.

Confocal imaging was executed on a Zeiss LSM 510 using a C-Apochromat 63× / 1.2 W corrected objective, 488-nm laser excitation, and 543-nm and 633-nm emission filters.

Results

Comparison with light microscopy. Glioblastoma exosomes, imaged by cathodoluminescence (Figure 5), appear as spherical bodies, falling within the size range measured by other techniques and were observed to bind to the membrane extensions (veils) of monocytes. The same type of cell, in the same experimental procedure (except for the addition of the cytoplasmic dye CMFDA [Invitrogen]), was mounted on a coverslip dish, rather than the aluminum, and imaged by confocal microscopy (Figure 6). In this case the exosomes are not individually resolvable nor is their association with the monocyte veils apparent—a difficulty we have consistently encountered in our confocal studies.

Glioblastoma exosomes were also fixed during the process of release from the tumor cell (Figure 7). Although during early cell culture we've imaged the protein EGFr covering the entire tumor cell, after several days of growth, the protein concentrates into exosomal structures, which pinch off of the cell surface.

As a demonstration of a different type of cell surface labeling, we used the surface protein CD14 of human monocytes. Cathodoluminescence images of these monocytes, labeled with Qdot 605 bound to anti-CD14 (Figure 8) show a high concentration of the protein on the membrane veils (sheet-like extensions of the surface membrane), especially on the veil edges. This is consistent with previous studies [23] that show the veils as the active site of T-cell binding and the location of high concentrations of other T-cell-interacting proteins.

Fluorophores. We have tested materials as diverse as phosphors, green fluorescent protein (GFP), quantum dots, and the common fluorescent tags attached to antibodies and proteins (Figure 9). All have responded well in this system though with variable stability under the electron beam and quantum yield (the ratio of photons emitted to photons absorbed). The common organic fluorescent dyes readily bleach under the conditions used here, whereas quantum dots have shown excellent stability. At 10–20 nm in diameter they are about the size of fluorescent proteins, are available in an extensive library of bioconjugates, and have been repeatedly proven effective [12].

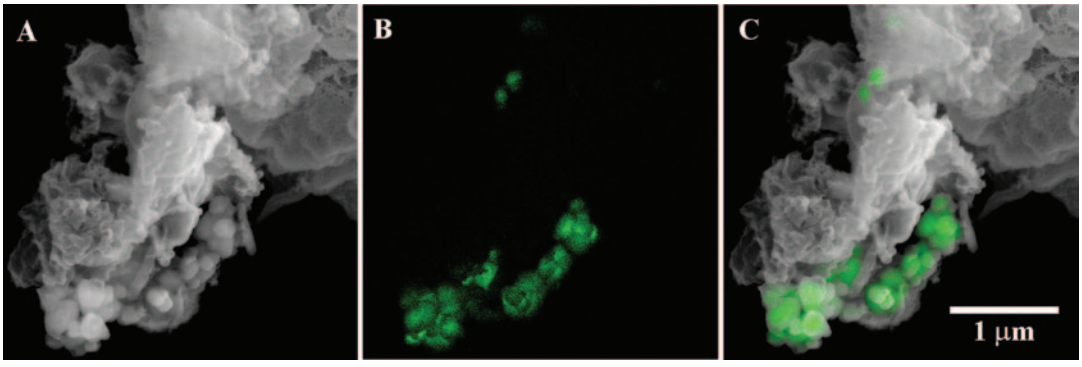

Figure 5: Tumor cell exosomes (green, B & C) adhere to the membrane extension of a monocyte. (A) Electron image (a mix of upper and lower detectors). (B) CL image of fluorescent Qdot 565 bound to anti-EGFr (see Cell Handling & Labeling). (C) Overlay of A & B. Scale bar = 1 mm.

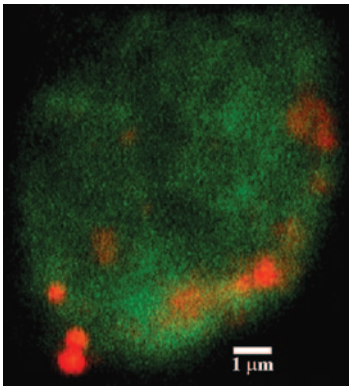

Figure 6: Confocal image of the same cell type as in Figure 5 prepared by the same protocol except for the addition of CMFDA (green) to the cell cytoplasm. Red Qdots 605, bound to anti-EGFr, light up the exosomes in this image.

Discussion

With cathodoluminescence imaging of fluorophores attached to specific antibodies on tumor cells, we have caught the release of exosomes and their subsequent attachment to the membrane veil-like structures of monocytes. Further studies with cathodoluminescence may reveal a time-dependent change of location of these exogenous bodies on or within the monocyte and, possibly, subsequent changes in the morphology of the monocyte itself. In addition, we were able to see that, coincidentally with release of exosomes from the tumor cells, EGFr concentrations on the cell surface changed. In a correlative study this technique has revealed that the primary location of the monocyte surface protein CD14 is on the membrane veils, which suggests an extensive role for the veils in the monocyte physiology. We were unable to capture any of these morphologically specific states by confocal light microscopy.

The resolution of field-emission SEM is currently reported at better than 1 nm [24, 25]. This, and the high quantum yield and submicron (15–20 nm) size of quantum dots and other new protein tags, along with the broad availability of fluorescent labels, will ultimately allow extensive morphological mapping of cell structures.

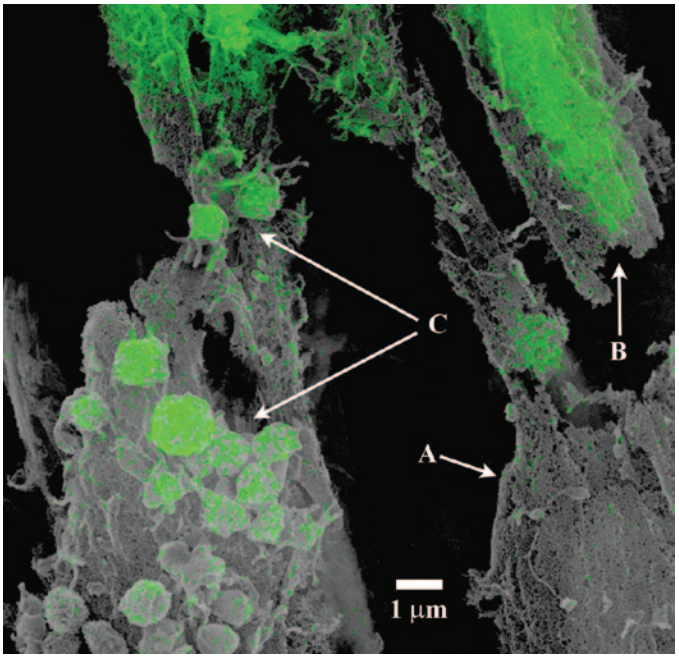

Figure 7: Developing exosomes on the cultured U373 glioblastoma tumor cell surface. Qdot 565 bound to anti-EGFr (green). (A) Cell with little EGFr on the surface. (B) Cell with large coverage of EGFr remaining. (C) Exosomes with EGFr on the surface of the cells.

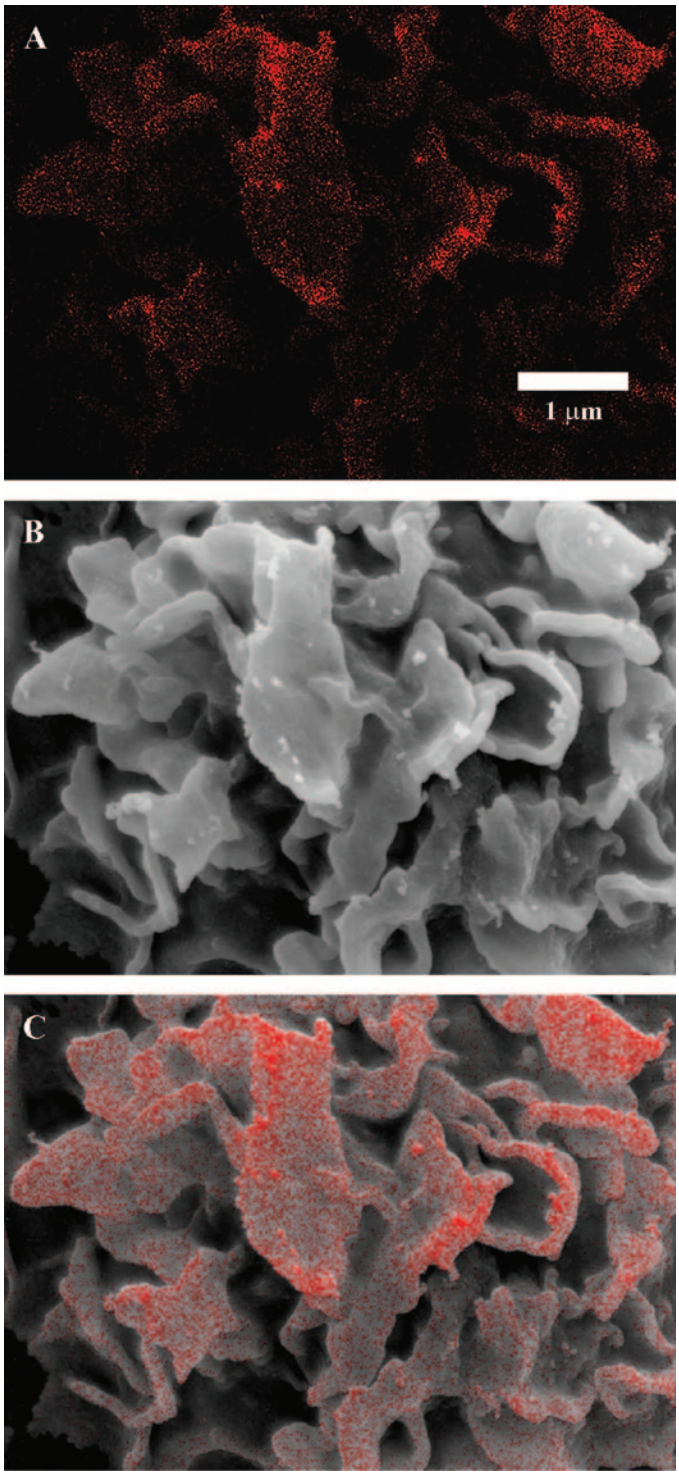

Figure 8: The surface of a highly veiled monocyte labeled with mouse anti-Human CD14/anti-mouse Qdot 605 (red), which is concentrated on the veil edges. (A) CL image. (B) Electron image from a mix of the upper and lower detectors. (C) Overlay of A and B. Scale bar = 1 mm.

With currently available SEM/CL instrumentation, multiple labels can be imaged on a single sample [26]. Thus, this technique could also be applied to determining the relative orientations of functionally interactive molecules such as receptors, ion barriers, molecularly selective membrane pores, or cell synapses. It might also be used in determining

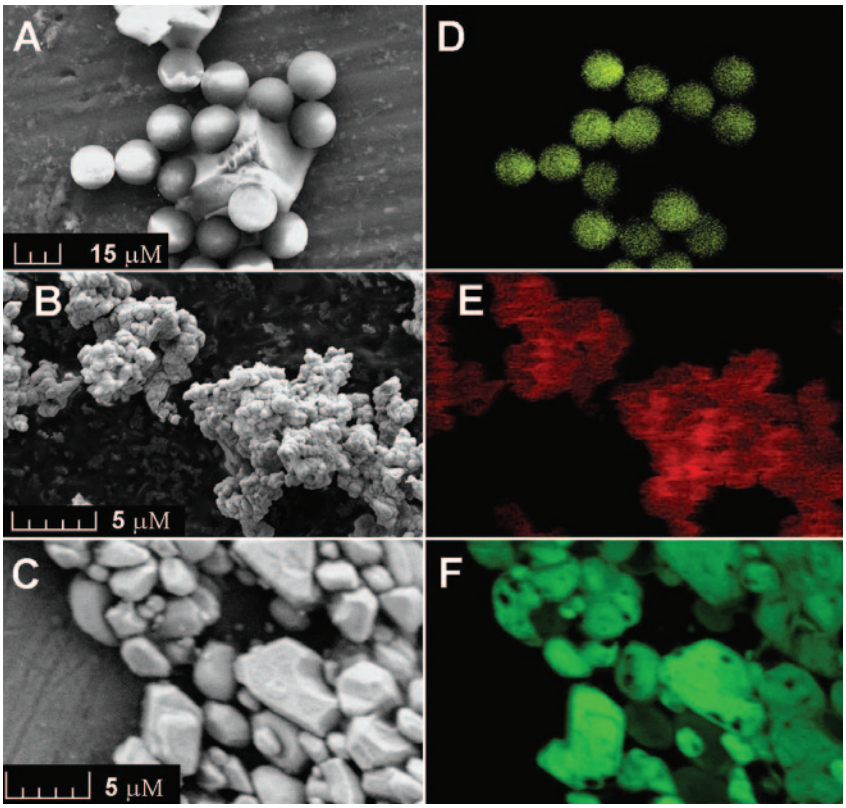

Figure 9: Fluorescence materials used as standards. (A, D) Fluoresbrite carboxylate microspheres (Polysciences, Inc., Warrington, PA), ex. 529 nm. (B, E) Y_2O_3:Eu red phosphors (Oxnica Inc., Mountain View, CA). (C, F) GFP isolated from *Aequorea forskålea* [28]. (A, B, C) Electron images. (D, E, F) CL images.

the morphological/protein health of a cell and relevance of this to the failure of certain intercellular processes. We might also find it being applied to the tracking of cell growth and cell placement in tissue reconstruction with the use of cloned fluorophores lighting up new daughter cells. We look forward to the time when all the known surface proteins of the monocyte, as well as other cells, can be mapped at various stages of cellular differentiation, action, and life.

Conclusions

We have shown the value of cathodoluminescence in tracking the transfer of material from one cell to another, the placement of exogenous material on a cell, and the rearrangement of molecular concentrations on a cell surface. Exosomes, isolated from a U373 glioblastoma tumor culture and incubated with human monocytes, were shown to bind to the veils of the monocytes, in some cases retaining individual exosomal structure, and, in other cases, fusing into extended areas of the cell. In addition, differences in the overall tumor cell coverage by the surface protein EGFr and the concentration of this protein on developing exosomal structures were captured by cathodoluminescence. We were also able to show that the monocyte protein CD14 is found predominantly on the edges of the cell membrane veils. Future studies with other proteins relevant to the function of these cells will give us a strong footing for exploring the role of monocytes in tumor control.

References

[1] R Bleher, I Kandela, DA Meyer, and RM Albrecht, *Journal of Microscopy* 230 (2008) 388–95.

[2] T Takizawa, K Suzuki, and JM Robinson, *J Histochem Cytochem* 46 (1998) 1097–1102.

[3] GM Venturi, L Tu, T Kadono, AI Khan, Y Fugimoto, P Oshel, CB Bock, AS Miller, RM Albrecht, P Kubes, DA Steeber, and TF Tedder, *Immunity* 19 (2003) 713–24.

[4] IK Kandela, R Bleher, and RM Albrecht, *J Histochem Cytochem* 55 (2007) 983–90, 2007, *%R 10.1369/jhc.6A7124.2007.*

[5] PJ Fisher, WS Wessels, AB Dietz, and FG Prendergast, *Optics in Life Sciences* 281 (2008) 1901–08.

[6] PV Hough, WR McKinney, MC Ledbeter, RE Pollack, and HW Moos, *P Natl Acad Sci USA* 73 (1976) 317–21.

[7] EF Bond, D Beresford, and GH Haggis, *Journal of Microscopy* 100 (1974) 271–82.

[8] MD Muir and PR Grant, *Cathodoluminescence*, Academic Press, London, 1974.

[9] T Mayr, "Database of Fluorescent Dyes, Properties and Applications," Graz University of Technology, 2005. http://www.fluorophores.tugraz.at/BrowseSubstance.php (accessed July, 2010).

[10] WC Chan and S Nie, *Science* 281 (1998) 2016–18.

[11] N Panchuk-Voloshina, RP Haugland, J Bishop-Stewart, MK Bhalgat, PJ Millard, F Mao, WY Leung, and RP Haugland, *J Histochem Cytochem* 47 (1999) 1179–88.

[12] Markmonitor Inc. "Qdot Nanocrystal Technology Overview," Invitrogen by Life Technologies. http://www.invitrogen.com/site/us/en/home/brands/Molecular-Probes/Key-Molecular-Probes-Products/Qdot/Technology-Overview.html (accessed January, 2010).

[13] J Skog, T Wurdinger, S van Rijn, DH Meijer, L Gainche, WT Curry, BS Carter, AM Krichevsky, and XO Breakefield, *Nat Cell Biol* 10 (2008) 1470–76.

[14] T Morimura, C Neuchrist, K Kitz, H Budka, O Scheiner, D Kraft, and H Lassmann, *Acta Neuropathologica* 80 (1990) 287–94.

[15] N Normanno and A De Luca, *J Clin Oncol* 23 (2005) 3866–67, *%R 10.1200/JCO.2005.05.233.*

[16] V-P Stanimir, AB Peggy, L Yi, Q Rui, LS Carol, Z Xinghua, and BD Allan, *The Prostate* 70 (2010) 443–55.

[17] E Stanley, Wright Cell Imaging Facility, "Autofluorescence: Causes and Cures." University Health Network, Toronto Western Research Institute, Toronto, ON. http://www.uhnres.utoronto.ca/facilities/wcif/PDF/Autofluorescence.pdf (accessed June, 2010).

[18] WA Barnett, ML Wise, and EC Jones, *Journal of Microscopy* 105 (1975) 299–303.

[19] PPH Cheng, D Silvester, G Wang, G Kalyuzhny, A Douglas, and RW Murray, *J Phys Chem B* 110 (2006) 4637–44.

[20] RD Powell, CMR Halsey, E Gutierrez, JF Hainfeld, and FR Furuya, "Dual-Labeled Probes for Fluorescence and Electron Microscopy," in *Proceedings of the fifty-sixth*

Annual Meeting, Microscopy Society of America, GW Bailey, KB Alexander, WG Jerome, M Bond, and J McCarthy, eds., Springer, New York, 1998.
[21] S Kirsch, Electron Microscopy Sciences, "Critical Point Drying Principles," Electron Microscopy Sciences, Hatfield, PA. http://www.emsdiasum.com/microscopy/products/equipment/critical_drying.aspx (accessed April, 2010).
[22] SO Kucheyev, M Toth, MR Phillips, JS Williams, and C Jagadish, *Appl Phys Lett* 79 (2001) 2154–56.
[23] PJ Fisher, P Bulur, AS Vuk-Pavlovic, FG Prendergast, and AB Dietz, *Blood* 112 (2008) 5037–45.
[24] J Villarrubia, *J Res Natl Inst Stan*, 107 (2002) 379.
[25] WL Chu, "Hitachi breaks SEM resolution barrier," LabTechnologist.com, http://www.labtechnologist.com/Products/Hitachi-breaks-SEM-resolution-barrier (accessed February, 2010).
[26] Network Solutions, LLC., "Cathodoluminescence." Gatan Inc. http://www.gatan.com/products/sem_products/products/cathodo/MonoCL3.php (accessed January, 2010).
[27] RB Gennis, *Biomembranes, Molecular Structure and Function,* Springer-Verlag, New York, 1989.
[28] FG Prendergast and KG Mann, *Biochemistry* 17 (1978) 3448–53.

MT

https://doi.org/10.1017/S1551929510000805 Published online by Cambridge University Press